RESEARCH ARTICLE | JANUARY 29 2025

Electrical conductivity of multilayered Cu/Nb composites fabricated by accumulative roll bonding

J. Justice ; A. Bauyrzhan; Y. Wang ; M. Khafizov ; J. Y. Cheng ; N. A. Mara ; S. Mishra ; F. Ronning ; O. Anderoglu

J. Appl. Phys. 137, 045105 (2025)
https://doi.org/10.1063/5.0222843

Journal of Applied Physics ARTICLE pubs.aip.org/aip/jap

Electrical conductivity of multilayered Cu/Nb composites fabricated by accumulative roll bonding

Cite as: J. Appl. Phys. **137**, 045105 (2025); doi: 10.1063/5.0222843
Submitted: 10 June 2024 · Accepted: 7 January 2025 ·
Published Online: 29 January 2025

J. Justice,[1] A. Bauyrzhan,[1,2] Y. Wang,[3] M. Khafizov,[3] J. Y. Cheng,[4] N. A. Mara,[4] S. Mishra,[5] F. Ronning,[5] and O. Anderoglu[1,a)]

AFFILIATIONS

[1]Department of Nuclear Engineering, University of New Mexico, Albuquerque, New Mexico 87131, USA
[2]Department of Nuclear Engineering, North Carolina State University, Raleigh, North Carolina 27695, USA
[3]Department of Mechanical and Aerospace Engineering, Ohio State University, Columbus, Ohio 43210, USA
[4]Department of Chemical Engineering and Materials Science, University of Minnesota, Minneapolis, Minnesota 55455, USA
[5]Los Alamos National Laboratory, Los Alamos, New Mexico 87545, USA

[a)]**Author to whom correspondence should be addressed:** oanderoglu@unm.edu

ABSTRACT

The electrical conductivity of nanolayered copper/niobium composites fabricated using accumulative roll bonding was investigated as a function of layer thickness. Cu/Nb was used as a model system to evaluate the processing-structure–property relationship stemming from the accumulative roll bonding process. The physical properties were compared against samples of individual average layer heights ranging from 193 to 25 nm. The electrical resistivity was measured over a temperature range of ∼3–300 K. Analysis on the role of interfaces on temperature dependence is conducted including the residual resistivity ratio and temperature coefficient of resistivity. It was found that electrical resistivity increases with decreasing layer height.

I. INTRODUCTION

Multilayered composite materials have shown remarkable properties such as very high strength even at elevated temperatures, high thermal stability, and irradiation resistance.[1–3] Interfaces present in these materials block the motion of dislocations. Therefore, as the average layer thickness gets smaller the density of the barriers increases, producing Hall–Petch layer size effects on strength. While the strengthening mechanism changes to confined layer slip (CLS) below an average layer thickness of ∼100 nm and single dislocation penetration below ∼10 nm, the strength continues to increase.[4] On the other hand, the interfaces can also trap Frenkel pairs created during irradiation and therefore increase the radiation damage resistance of these composite materials.[2] Therefore, the density of interfaces plays a crucial role in these remarkable improvements for Cu/Nb nanolaminates, henceforth Cu/Nb, and various other bimetallic material combinations considered for various applications. However, the physical properties of multilayered materials fabricated by accumulative roll bonding (ARB) are not well researched. As a result, a fundamental understanding of the effect of these interfaces on properties such as electrical conductivity is important for practical applications where interface density may be tuned to give rise to improved performance. This work presents electrical properties of ARB-processed Cu/Nb nanolayered composites as a function of average layer thickness in the range of 193–25 nm.

The electrical properties of ARB Cu/Nb can be captured by the Fuchs–Sondheimer (F–S) model, which was first developed to understand resistivity in thin films.[5,6] This model was originally semi-classically derived by solving the Boltzmann kinetic equation under the understanding that in single layer thin films, the surface acts as a significant scattering source. This model has been used to understand the role of interfaces in nanolayered materials, where

the interfaces between layers are the scattering mechanism of interest.[7] However, the F–S model did not account for electron scattering off of grain boundaries, which produces non-negligible contributions to resistivity in other nanolayers produced by physical vapor deposition (PVD).[7]

Dimmich developed a model that combined interface and grain scattering in bimetallic nanolayered materials.[8] This model used the understanding of the F–S model, but combined the understanding of grain boundary scattering as described by the Mayadas and Shatzkes (M–S) model.[9] This proved invaluable for bimetallic nanolayered materials whose grain size was on the order of the mean free path of electrons in the bulk constituent metals. However, this combination results in a complicated numerical integral which is difficult to solve over a range of conditions and is seldom used in light of simpler models with adequate accuracy.

Edwards *et al.* resolved the Boltzmann kinetic equation for bimetallic nanolayered boundaries.[10] This model was successfully applied to Cu/Cr nanolayered materials.[11] While this model was developed for the geometry of the present study, the widespread use of the F–S model for nanolayered materials makes it the optimum choice in order to compare the structure–properties relations between nanolayered materials produced using PVD and ARB.

This study measures the electrical conductivity of ARB produced nanolaminates to investigate the role interfaces contribute to physical properties in bulk samples. Previous work on resistivity of Cu/Nb composites was limited to thin films. The present study focuses on bulk samples, whose electrical properties have yet to be investigated. Bulk samples also allow for investigation of properties normal to the interfaces, which is unable to be investigated in thin films. The residual resistivity ratio and temperature coefficient of resistivity are used to understand the relative contributions of interface scattering and electron–phonon scattering to determine the dominant scattering mechanisms. Comparisons to literature of nanolaminate composites produced by deposition are also conducted.

II. EXPERIMENTAL

Cu/Nb with individual layer thicknesses of 193, 100, 50, and 25 nm were made using ARB. This process involved repeatedly roll bonding a three-high stack of Cu–Nb–Cu until the layer height reached 193 nm. Afterward, the material was annealed at 800 °C to remove damage from cold working and sharpen the texture. Then specimens were further rolled until the desired layer height was achieved without re-stacking performed in the previous process. These specimens were longitudinally rolled (LR), such that the additional rolling occurred in the same direction as the original rolling. Another specimen of 25 nm average layer height was fabricated, however this one was cross-rolled (CR), where the additional rolling was done perpendicular to the initial rolling.[12] This results in the same average layer thickness as the 25 nm LR specimen but with different texture.

Electrical resistivity was measured using a standard four-probe method over a temperature range of 2–300 K. The material's resistivity, ρ, is defined by

$$\rho = R\frac{S}{d}, \tag{1}$$

where R is measured resistance, d is the distance between the electrodes, and S is the cross-sectional area. Specimens were machined to a rectangular size ~4.5 mm long. Pt wires were attached to the surface using a high conductive paste. Resistivity was measured in the roll direction (RD) for all specimens, and additionally in the normal direction (ND) for the 193 nm specimen.

III. RESULTS AND DISCUSSION

A. Microstructure

The microstructure was investigated using focused ion beam (FIB) microscopy in order to reveal the grain structure in addition to the layer structure. Figure 1 shows the microstructure of the 193 nm specimen. The ND and transverse direction (TD) are shown with the RD orthogonal to both directions. The nonuniformity in the layer structure is characteristic of the accumulative roll bonding processing. The pre-existing rolling textures in the Nb and Cu are sharpened due to the annealing process.[12]

Figure 1 shows spheroidized grains in the copper. The structure found in the FIB analysis is consistent with the SEM and EBSD results reported in Ref. 12. There is also significant layer discontinuity, and regions where the local layer height is significantly lower than the average layer height.

B. Electrical resistivity

The resistivity of metals is governed by the mobility of electrons which is impacted by electron scattering with defects. Matthiessen's rule can be applied to evaluate total resistivity of the metal as the sum of the individual scattering sources,[13]

$$\rho = \rho_b(T) + \rho_{df}(n_d) + \rho_s(h), \tag{2}$$

where ρ_b is the contribution from electron–phonon scattering, ρ_{df} is the contribution from point defects, and ρ_s is the contribution

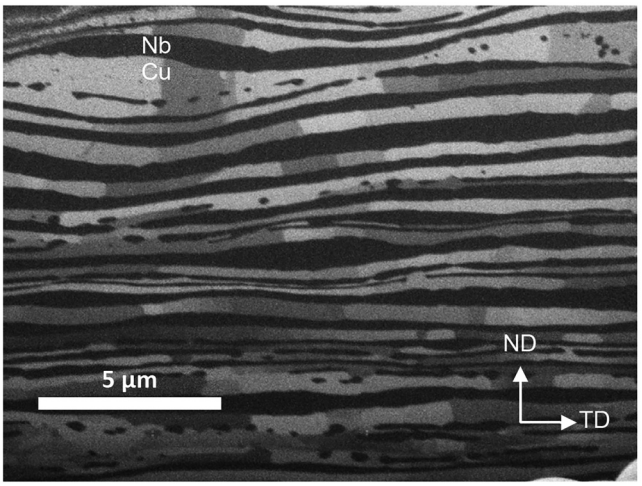

FIG. 1. Focused ion beam micrograph of the 193 nm specimen after annealing.

from interfaces. Thermal population of phonons increases with temperature, and these effects are the primary cause of the resistivity–temperature relationship.

Figure 2 shows the temperature dependence of the resistivity for various individual layer heights. The resistivity of the Cu/Nb multilayer composites increases with decreasing individual layer thickness due to a decrease in electron mobility. At sufficiently low temperatures, the composite resistivity vanishes, as niobium is a superconductor below a critical temperature of 9.3 K. This phenomenon is independent of the layer structure, as all current becomes shunted to the niobium layers once they become superconducting.

In order to better understand the contributions to resistivity caused by impurities, the Residual Resistivity Ratio (RRR) is used. Typically, the RRR is used to determine the relative amounts of impurity elements in a sample. However, the dominant contributor to residual resistivity are Cu/Nb heterophase interfaces in the present study since intralayer grain boundaries are much larger than layer thickness. Thus, comparing the RRR as a function of layer height shows the relative contribution of interfaces to the resistivity of the samples. The RRR is given by

$$\mathrm{RRR} = \frac{\rho_{300\,\mathrm{K}}}{\rho_0}, \tag{3}$$

where the RRR is the ratio of the resistivity at 300 K and the residual resistivity. Typically, the residual resistivity is taken at nearly 0 K. However, superconductivity nearly eliminates residual resistivity. Thus, the residual resistivity for this sample is instead defined as the resistivity slightly above the critical temperature of niobium. The low temperature behavior of metals is described by[14]

$$\rho = \rho_0 + JT^k, \tag{4}$$

where J and k are fitting constants, and ρ_0 is the residual resistivity at 10 K.

Figure 3 shows the RRR and the residual resistivity as a function of individual layer height. The residual resistivity shows a sharp decrease with layer height, while the RRR is linear with respect to layer height. Thus, the scattering site concentration is highly correlated with the interface density of the composite. The linear fit to the LR RRR had an R^2 of 0.9889. The CR specimen has a lower residual resistivity and a higher RRR than the LR specimen. This can be explained by the change in texture created by the cross-rolling process which in turn causes less scattering at the interface.

The temperature coefficient of resistivity (TCR) is used to quantify the relationship between resistivity and temperature. The TCR is defined and calculated by[8]

$$\alpha = \frac{1}{\rho}\frac{\mathrm{d}\rho}{\mathrm{dT}} \approx \frac{1}{\rho(150\,\mathrm{K})}\frac{\rho(300\,\mathrm{K}) - \rho(150\,\mathrm{K})}{300\,\mathrm{K} - 150\,\mathrm{K}}. \tag{5}$$

The TCR for bulk Cu and Nb is 0.029 and 0.0129 K^{-1}, respectively; for thin films, the TCR for Cu and Nb is 0.011 and 0.006 K^{-1}, respectively.[15] The TCR for bulk materials is higher than for thin films because the latter typically have a larger interface-to-volume ratio than the former and interface contribution to electron scattering is not temperature dependent.

Equations (2) and (5) imply that temperature sensitivity in resistivity is dominated by phonon–electron scattering. Interfaces can scatter and trap phonons,[7] but at high defect concentrations phonons trapping is favored.[16] Thus, the TCR decreases with increasing interface density. Figure 4 shows the TCR for the composites. The CR specimen has a higher TCR than the LR specimen partly because of its decreased resistivity. Because the interfaces are not as significant of scattering sources in the CR specimen, the relative contribution to the resistivity from temperature dependent

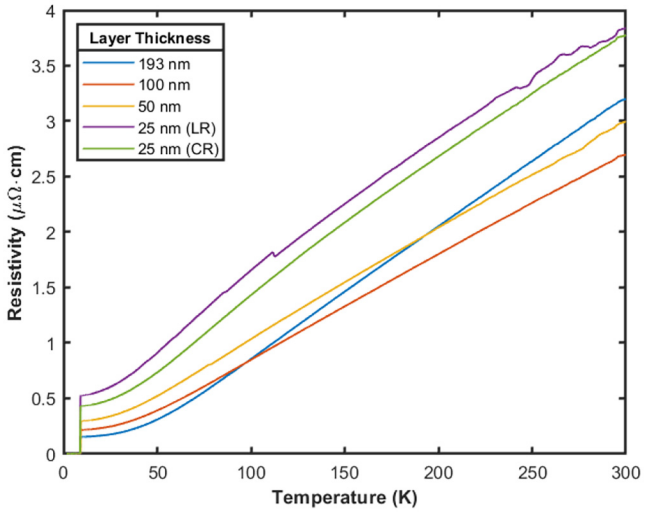

FIG. 2. Electrical resistivity as a function of temperature. The slope indicates the resistivity's sensitivity to temperature dependent scattering sources. Superconductivity is observed at a critical temperature of ~9.3 K.

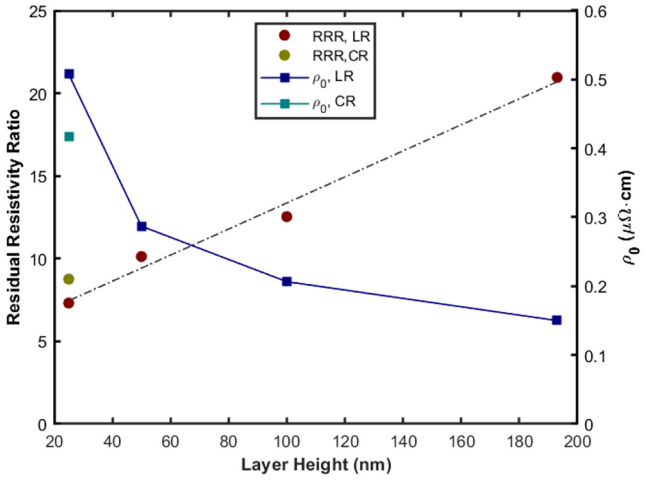

FIG. 3. A plot of RRR (left axis) and ρ_0 (right axis) with respect to temperature. A linear trend is observed between RRR and temperature, as shown by the dotted dashed line.

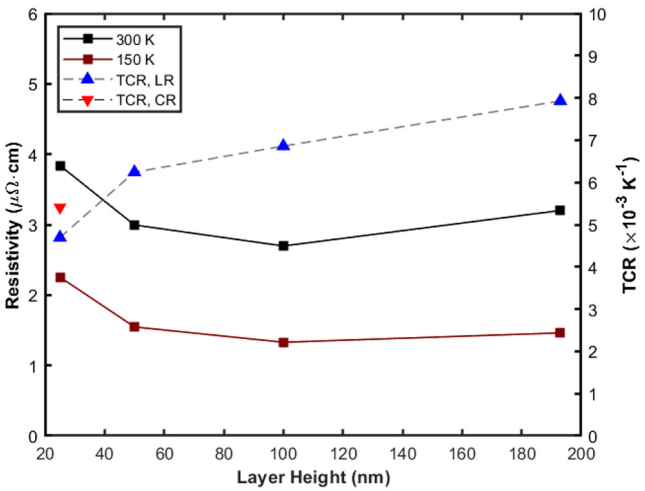

FIG. 4. TCR presented along with 150 and 300 K electrical resistivities as a function of layer height. TCR increases with increasing layer height.

scattering sources is higher. Therefore, the CR specimen has a higher TCR.

The Fuchs–Sondheimer (F–S) model is used to understand the relationship between layer height and resistivity. Fuchs determined that for thin films, the surface is a significant scattering source that leads to increased resistivity in the films compared to the bulk metal.[5] The F–S model is derived from a semi-classical solution to the Boltzmann equation and is given by[5,6]

$$\rho = \rho_0 \left[1 - \left(\frac{3}{2k} \right) (1-p) \int_1^\infty \left(\frac{1}{\varepsilon^3} - \frac{1}{\varepsilon^5} \right) \frac{1 - e^{-k\varepsilon}}{1 - pe^{-k\varepsilon}} d\varepsilon \right]^{-1}, \quad (6)$$

where ρ_0 here is the bulk resistivity, p is the fraction of electrons that scatter elastically at the interface, and k is the ratio of individual layer height and the intrinsic mean free path of the material. A value of $p = 0$ corresponds to completely diffuse electron reflection at interfaces, while a value of $p = 1$ corresponds to perfect specular reflection.

The temperature-dependent intrinsic mean free path of electrons can be determined for Cu and Nb by[15]

$$l = \frac{h}{2\pi} \frac{1}{e^2 \rho} \left(\frac{\sqrt{3}\pi}{n} \right)^{2/3}, \quad (7)$$

where h is Planck's constant, e is elementary charge, and n is the carrier density as reported in Ref. 17. The resistivity, ρ, is taken as the resistivity of Cu and Nb thin films 1 μm thick as reported in Ref. 15.

The applicability of Eq. (6) to the current work rests on a few assumptions. First, it is assumed that the bulk resistivity can be found by:[8]

$$\rho_0 = \frac{2\rho_{Cu}\rho_{Nb}}{\rho_{Cu} + \rho_{Nb}}. \quad (8)$$

The bulk resistivities of Cu and Nb were taken from Ref. 18. Second, p is assumed to be 0.5 as it is elsewhere in the literature.[7,15,19] Third, the mean free paths for Cu and Nb found in Eq. (5) were averaged and used in Eq. (4). The average mean free path is 18 nm. This is sufficiently smaller than the smallest layer height investigated, thus the Fuchs size limit, is not of interest. This limit is visualized in Fig. 5, where the resistivity asymptotically approaches infinity at $h = 0$.

Figure 5 shows resistivities predicted by the Fuchs–Sondheimer model at 300 K as a function of layer height. The resistivity trend shown in Fig. 5 closely matches measured resistivities. Wang *et al.* found that for PVD Cu/V films, the F–S model did not accurately predict the measured resistivity.[7] This is due to the difference in grain size and texture between nanolayered materials produced by PVD and ARB.[20] In the present study, the grain size is on the order of micrometers in the direction of the current flow. However, PVD often produces materials with nanometer size grains, the same order of magnitude as the mean free path of electrons.

Based on the analysis on electrical resistivity thus far, and the invariability of thermal conductivity of ARB Cu/Nb reported in Ref. 21, interfaces appear to be the dominant scattering source, instead of phonon–electron scattering or grain boundary scattering. This is evidenced by the reduction in electrical properties from bulk at temperatures near 300 K, where electron–phonon scattering typically dominates. In PVD Cu/Nb thin films, the surface also acts as a significant defect and scattering source due to the large surface area to volume ratio.

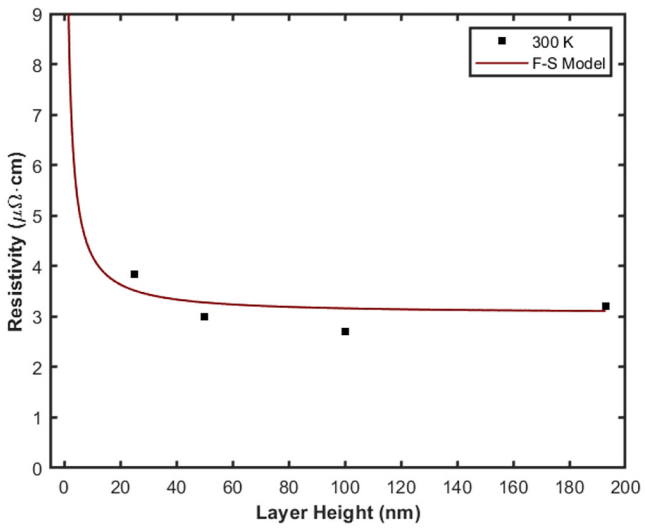

FIG. 5. Comparison of experimentally measured 300 K resistivities and F–S model predicted resistivities as a function of layer height.

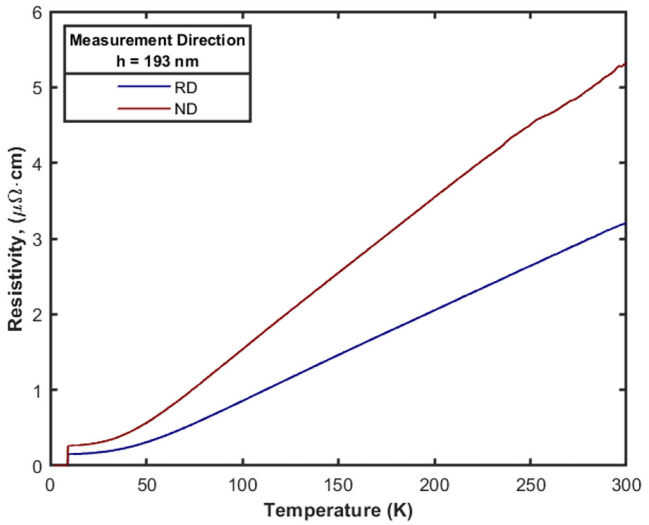

FIG. 6. Resistivity measured along RD and ND for $h = 193$ nm Cu/Nb as a function of temperature.

To determine the directional dependence on the resistivity, the 193 nm sample's resistivity was measured with current being driven in the ND. This can be compared to resistivity measurements presented in Figs. 2–4, where current was driven in the RD. This comparison is shown in Fig. 6. Notably, the ND direction has a higher resistivity and residual resistivity than the RD. However, the RRR and TCR of both only differ by a few percent. The TCR measured in the ND was 0.0073 K^{-1} while the TCR measured in the RD was 0.0079 K^{-1}. The RRR was 20.22 along ND and 20.96 along RD. This indicates that resistivity has a similar relative contribution from temperature sensitive scattering sources along ND and RD.

Superconductivity is present along both ND and RD, which is consistent with the ~39 nm coherence length for superconductivity in niobium.[22] Thus, so long as there is a single point in each Cu layer where the local layer thickness is 39 nm or less, then superconductivity can occur. Current can shunt along superconducting niobium along ND since Cu and Nb layers contain discontinuities as seen in Fig. 1. This extreme reduction in local layer height from the average layer height has implications for the thermal stability of ARB Cu/Nb composites at high temperatures. When layer height becomes extremely small, the thermal stability has been shown to weaken.[23] Thus, even at a relatively large average layer height, localized regions of the material may not exhibit high thermal stability.

IV. CONCLUSIONS

The electrical conductivity of nanolayered composites fabricated by accumulative roll bonding was measured for the first time in literature. The electrical resistivity–temperature response was measured from ~3 to 300 K. It was found that the specimens have a significant reduction in their TCR from bulk, due to the dominance of heterophase interfaces as the primary scattering mechanism. The resistivity–average layer height relationship was compared to resistivities predicted by the Fuchs–Sondheimer model. Experiments and theoretical predictions agreed remarkably due to the large in-layer grain size. Heterophase interfaces produce outsize effects on electrical conductivity, demonstrating their importance when considering charge carrier transport in bulk composites.

ACKNOWLEDGMENTS

J. Justice acknowledges financial support from the Nuclear Science and Security Consortium. This material is based upon work supported by the Department of Energy National Nuclear Security Administration through the Nuclear Science and Security Consortium under Award No. DE-NA0003996. Y. Wang. and M. Khafizov acknowledge support from the Center for Thermal Energy Transport under Irradiation, an Energy Frontier Research Center funded by the U.S. DOE, Office of Science, Basic Energy Sciences. J. Y. Cheng was supported in part by DOE NNSA SSGF under Cooperative Agreement No. DE-NA0003960. N. A. Mara gratefully acknowledges support from project DE-SC0020133 Office of Science, Basic Energy Sciences. Resistivity measurements at LANL were supported by the U.S. DOE Basic Energy Sciences, Division of Materials Science and Engineering project "Quantum fluctuations in narrow-band systems." This research was partly supported by Nuclear Energy University Program Grant No. DE-NE0008656.

AUTHOR DECLARATIONS

Conflict of Interest

The authors have no conflicts to disclose.

Author Contributions

J. Justice: Formal analysis (equal); Writing – original draft (equal); Writing – review & editing (equal). **A. Bauyrzhan:** Formal analysis (supporting). **Y. Wang:** Methodology (equal). **M. Khafizov:** Methodology (equal). **J. Y. Cheng:** Writing – review & editing (supporting). **N. A. Mara:** Conceptualization (supporting). **S. Mishra:** Methodology (equal). **F. Ronning:** Methodology (equal). **O. Anderoglu:** Conceptualization (lead); Supervision (lead); Writing – review & editing (lead).

DATA AVAILABILITY

The data that support the findings of this study are available from the corresponding author upon reasonable request.

REFERENCES

[1]A. Misra, M. J. Demkowicz, X. Zhang, and R. G. Hoagland, J. Mater. **59**, 62–65 (2007).
[2]M. J. Demkowicz, R. G. Hoagland, and J. P. Hirth, Phys. Rev. Lett. **100**(13), 136102 (2008).
[3]L. F. Zhang, R. Gao, J. Hou, B. L. Zhao, M. Sun, T. Hao, Z. M. Xie, R. Liu, X. P. Wang, Q. F. Fang, and C. S. Liu, J. Nucl. Mater. **543**, 152548 (2021).
[4]A. Misra, J. P. Hirth, and R. G. Hoagland, Acta Mater. **53**(18), 4817–4824 (2005).
[5]K. Fuchs, Math. Proc. Cambridge Philos. Soc. **34**(1), 100–108 (1938).
[6]E. H. Sondheimer, Adv. Phys. **1**(1), 1–42 (1952).

[7]P. P. Wang, X. J. Wang, J. L. Du, F. Ren, Y. Zhang, X. Zhang, and, E. G. Fu, Acta Mater. **126**, 294–301 (2017).
[8]R. Dimmich, J. Phys, F **15**, 2477–2487 (1985).
[9]A. F. Mayadas and M. Shatzkes, Phys. Rev. B **1**(4), 1382–1389 (1970).
[10]D. M. Edwards, J. Mathon, and R. B. Muniz, IEEE Trans. Magn. **27**(4), 3548–3552 (1991).
[11]A. Misra, M. F. Hundley, D. Hristova, H. Kung, T. E. Mitchell, M. Nastasi, and J. D. Embury, J. Appl. Phys. **85**, 302–309 (1999).
[12]J. Y. Cheng, M. Radhakrishnan, C. Miller, R. Mier, S. C. Vogel, D. J. Savage, J. S. Carpenter, O. Anderoglu, and N. A. Mara, Mater. Sci. Eng. A **886**, 145610 (2023).
[13]C. Kittel, *Introduction to Solid State Physics* (John Wiley & Sons, inc, 2005).
[14]P. K. Moussouros and J. F. Kos, Can. J. Phys. **55**, 2071–2079 (1977).
[15]M. Fenn, G. Akuetey, and P. E. Donovan, J. Phys.: Condens. Matter **10**, 1707–1720 (1998).
[16]S. K. Estreicher, T. M. Gibbons, B. Kang, and M. B. Bebek, J. Appl. Phys. **115**(1), 012012 (2014).
[17]N. W. Ashcroft and N. D. Mermin, *Solid State Physics* (Holt, Rinehart and Winston, New York, 1976).
[18]F. Cardarelli, *Materials Handbook: A Concise Desktop Reference*, 3rd ed. (Springer, 2018).
[19]W. Zhang, S. H. Brongersma, O. Richard, B. Brijs, R. Palmans, L. Froyen, and K. Maex, Microelectron. Eng. **76**(1–4), 146–152 (2004).
[20]S. B. Lee, J. E. LeDonne, S. C. V. Lim, I. J. Beyerlein, and A. D. Rollett, Acta Mater. **60**(4), 1747–1761 (2012).
[21]J. Justice, University of New Mexico (2023).
[22]B. W. Maxfield and W. L. McLean, Phys. Rev. **139**(5A), A1515–A1522 (1965).
[23]J. S. Carpenter, S. J. Zheng, R. F. Zhang, S. C. Vogel, I. J. Beyerlein, and N. A. Mara, Philos. Mag. **93**(7), 718–735 (2013).